

Interleaved Dual NMR Acquisition of Equivalent Transfer Pathways in TOCSY and HSQC Experiments

Pau Nolis,^[a] Kumar Motiram-Corral,^[a] Míriam Pérez-Trujillo,^[a] and Teodor Parella^{*[a]}

A dual NMR data acquisition strategy to handle and detect two active equivalent transfer pathways is presented and discussed. We illustrate the power of this time-efficient approach by collecting two different 2D spectra simultaneously in a single experiment: i) TOCSY or HSQC-TOCSY spectra with different mixing times, ii) F2-¹³C-coupled and decoupled HSQC spectra, iii) conventional and pure-shift HSQC spectra, or iv) complementary HSQC and HSQC-TOCSY spectra.


The overall experimental time of a 2D NMR experiment is defined fundamentally by the imposition of extended recycle delays for a proper T_1 relaxation, of an enough number of recorded t_1 increments to achieve an optimum resolution in the indirect F1 dimension and/or of a minimum number of scans per t_1 increment required to complete a phase cycle for efficient coherence transfer pathways (CTP) selection. This situation is commonly found in modern NMR applications on small molecules, where some milligrams of sample are often more than enough to run the most basic experiments in short experimental times. Possible solutions to economize spectrometer time could be the attempt to speed up data acquisition by some fast NMR method, including shortening the recycle delay, the collection of a moderate number of t_1 increments or the efforts to reduce the needs of long phase cycles by using pulsed field gradient (PFG) CTP selection. Another option relies on the acquisition of multiple NMR spectra using a single pulse sequence which can offer attractive benefits regarding simplicity, efficiency, automation and, in some cases, improved sensitivity per time unit. Some examples of this multiple data acquisition strategy include the collection of multiple FIDs within the same scan (MFA),^[1–3] the recent concept of NOAH based on the interleaved acquisition of various experiments to avoid long recycle delays,^[4,5] the simultaneous acquisition of equivalent ¹³C and ¹⁵N spectra by time-sharing NMR spectroscopy,^[6] or the use of multiple receivers to detect different nuclei in a parallel or interleaved manner.^[7] The simultaneous acquisition of multiple spectra is particularly useful when dealing on complementary NMR experiments having comparable sensitivity (requiring similar scans per t_1 increments, similar

phase cycling), resolution (similar number of t_1 increments) and/or performance (similar parameters settings, the same acquisition mode...) requirements. The success of these time-efficient methods depends on which is the best multiple acquisition strategy (parallel, interleaved, afterglow, separate...) regarding sensitivity, performance and/or spectrometer time savings.

On the other hand, NMR pulse sequences usually monitor a specific CTP by an appropriate phase cycle or PFG coherence selection procedure. However, some sequences have been designed to exploit several CTPs at the same time. A very representative example is the so-called Preservation of Equivalent Pathways (PEP) technique which has been used to add up two different co-existing magnetization components in a single NMR experiment. For instance, PEP has been successfully applied to enhance the sensitivity by a theoretical factor of 2 (signal-to-noise (SNR) ratio by 1.4-fold) during the same total acquisition time in 2D TOCSY,^[8,9] 2D HMQC,^[10,11] 2D HSQC^[12–16] and 2D HSQC-TOCSY^[17–20] experiments or has also been used to generate spin-state selective states in TROSY-type experiments.^[21–24] Both PEP and TROSY elements are standard building blocks in many multidimensional experiments,^[25] but it is worth mentioning that such theoretical sensitivity gains are only achieved for CH and NH spin systems, but not for CH₂ or CH₃ signals.

Here we show how the two CTPs components involved in PEP-based experiments can be managed and detected separately by using the time-optimized MFA technique. As a proof of concept, the features of this method are described, including a discussion about the increased information content, the relative sensitivities for each collected component and the benefits concerning spectrometer times achieved for such an approach. To start, we have chosen the sensitivity-enhanced version of the TOCSY (SE-TOCSY) experiment using a z-filtered DIPSI-2 as the isotropic mixing transfer for propagation between J coupled protons (Figure 1A).^[26] The SE-TOCSY sequence also incorporates gradient-enhanced CTP selection based on the well-known echo/anti-echo acquisition and processing protocols to provide pure absorption lineshapes.^[9] The high sensitivity of the TOCSY experiment makes it suitable for the rapid and successful application on any molecules, only requiring some milligrams of sample and two scans per t_1 increment. Two magnetization components (I_x and I_y) present just before the DIPSI-2 scheme contribute equally to the detected signal after the last 90° ¹H pulse in SE-TOCSY. We propose to insert a simple NMR element consisting of an FID period followed by a purging G2 gradient into the SE-TOCSY sequence to manipulate these orthogonal components selec-

[a] Dr. P. Nolis, K. Motiram-Corral, Dr. M. Pérez-Trujillo, Dr. T. Parella
Servei de Resonància Magnètica Nuclear
Universitat Autònoma de Barcelona
E-08193 Bellaterra, Barcelona, Catalonia
E-mail: Teodor.parella@uab.cat

 Supporting information for this article is available on the WWW under
<https://doi.org/10.1002/cphc.201801034>

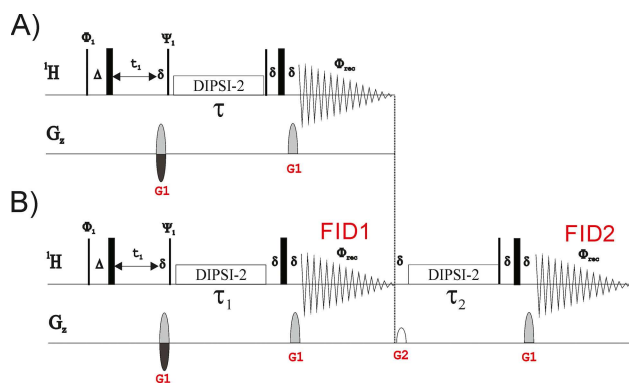


Figure 1. Pulse schemes of the A) conventional 2D sensitivity- and gradient-enhanced TOCSY (SE-TOCSY) and B) MFA-TOCSY/TOCSY experiments.

tively. Figure 1B shows the pulse scheme of the novel MFA-TOCSY/TOCSY experiment which can be used to obtain two 2D TOCSY spectra with different mixing times. The first FID acquisition period (FID1) is designed to observe exclusively transverse I_x components generated during the τ_1 mixing time, whereas the other I_z component remains non-observable. After that, the purging G2 gradient is applied to remove any residual transverse magnetization, and a subsequent 90° pulse flips the unexploited I_z component to the transverse plane to be acquired during a second acquisition period (FID2) inserted after another TOCSY transfer. This method allowed the single-shot dual acquisition of two different TOCSY experiments sharing the same variable t_1 period but recorded with two different mixing times (τ_1 and τ_2 , respectively).

Figure 2 shows the regular SE-TOCSY ($\tau = 60$ ms) acquired in 10 m 28 s, and the two TOCSY spectra both acquired in a total

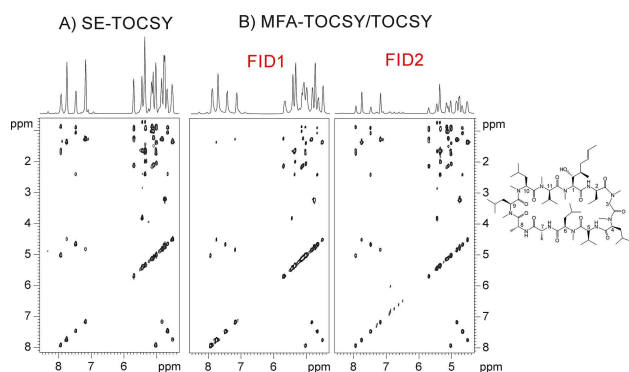


Figure 2. 2D TOCSY spectra of cyclosporine obtained from the A) SE-TOCSY ($\tau = 60$ ms; experimental time = 10 m 28 s) and B) MFA-TOCSY/TOCSY (overall experimental time for both spectra = 11 m 16 s) experiments. Mixing times in the MFA-TOCSY/TOCSY were $\tau_1 = 20$ ms (FID1) and $\tau_2 = 60$ ms (FID2). 1D slices show the internal positive projection for each 2D spectrum.

experimental time of 11 m 16 s (only 7.6% of additional spectrometer time; see Table S1 in SI) with the MFA-TOCSY/TOCSY sequence, with mixing times of $\tau_1 = 20$ ms (FID1) to observe short-range connectivities and $\tau_2 = 60$ ms (FID2) to

trace out longer correlations, respectively. In all these experiments, 1024 points were collected in each acquisition (TD2) giving an acquisition time (AQ) of 102 ms for each FID1 and FID2 periods. As expected, FID1 shows about the 50% of the signal detected in the equivalent SE-TOCSY acquired under identical conditions. The proposed MFA approach can induce two interferences in the second FID2: a relative sensitivity loss due to diffusion effects and the potential presence of NOE and NOE-related contributions. In practice, the second TOCSY spectra show a decreased sensitivity due to the diffusion effects generated by the long distance between the defocusing and refocusing gradients. However, the sum of the positive projection FID1 + FID2 only shows a minimum decrease in sensitivity about 15–20% with respect to the maximum expected for the SE-TOCSY (Figure S2). Such losses are negligible for everyday applications, but the TOCSY version without PFG selection^[8] could be used to avoid them. On the other hand, NOE and NOE-related contributions could be distinguished by their relative opposite phase but their intensities become not relevant for small molecules in the mentioned conditions.

The separate handling of the PEP components can also be implemented in the sensitivity- and gradient-enhanced HSQC-PEP (SE-HSQC) experiment shown in Figure 3A. Equation (1) summarizes their evolution for an isolated CH spin system after the t_1 period:

$$\begin{aligned}
 2I_zS_x + 2I_zS_y &\xrightarrow{90^\circ(H,x)-90^\circ(S,x)} 2I_yS_x + 2I_yS_z \xrightarrow{\Delta-180^\circ(H,x)-180^\circ(S,x)-\Delta} \\
 2I_yS_x + I_x &\xrightarrow{90^\circ(H,y)-90^\circ(S,y)} 2I_yS_z + I_z(\text{point a}) \xrightarrow{\Delta-180^\circ(H,x)-180^\circ(S,x)-\Delta} \\
 I_x + I_z(\text{point b}) &\xrightarrow{90^\circ(H,x)} I_x + I_y(\text{point c})
 \end{aligned}
 \quad (1)$$

There are three key points to highlight in the PEP scheme. In point a, only an anti-phase (AP) term is observable while the other component resides in the z-axis; in point b, only the corresponding in-phase (IP) magnetization remains observable after the subsequent refocusing period; in point c, both signals become observables as orthogonal IP states. The SE-HSQC pulse sequence is specifically designed to generate these two in-phase contributions, which are added up to offer a sensitivity enhancement of 2 compared to the alternative application of a single-echo INEPT refocusing in HSQC. However, this sensitivity gain is not general for all CH_n multiplicities. Only when the inter-pulse Δ_1 and Δ_2 delays are set to $1/4 J$, a maximum theoretical enhancement is expected just for CH spin systems (signal-to-noise (SNR) ratio by 1.4-fold).

The approach followed in this work is different to other previous MFA experiments which use the so-called afterglow magnetization. We explain how these two PEP components can be handled differently, not to mix them in a single acquisition but separating them to provide two different datasets. Figure 3B displays a general MFA-HSQC/HSQC pulse scheme developed to monitor each PEP component. As a first option, only one of the two magnetization components can be selectively detected by activating data acquisition at points a or b, either as AP signals or IP after proper refocusing, respectively,

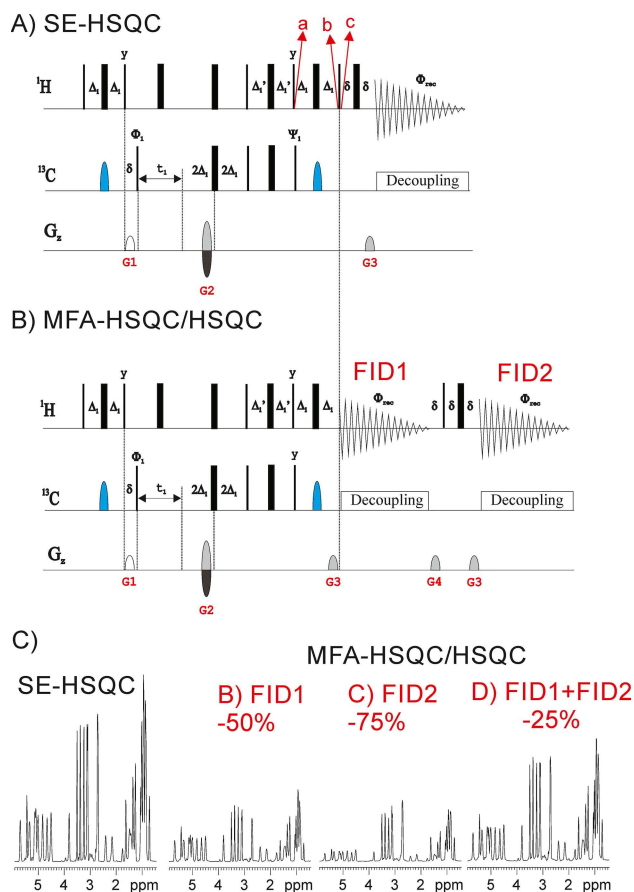


Figure 3. Pulse schemes of the A) conventional sensitivity- and gradient-enhanced HSQC (SE-HSQC) and B) MFA-HSQC/HSQC experiments. C) Relative sensitivities achieved in MFA experiments. Positive projections corresponding to (left) SE-HSQC, (center) FID1 and FID2 of the MFA-HSQC/HSQC spectra, respectively, and (right) the sum of FID1 and FID2.

while the second component remains non-observable as I_z . After this FID1, a purging G4 gradient is applied to remove any residual transverse magnetization from the first component and followed by a $90^\circ(^1\text{H})$ pulse to create transverse IP magnetization from the unexploited second component. At this new point c, a new acquisition period is inserted (FID2) to detect it after applying a refocusing gradient.

To analyse the performance of our approach, we have applied the MFA-HSQC/HSQC experiment to obtain a 2D HSQC spectrum in both FID1 and FID2 and compare them to SE-HSQC with respect to real sensitivity and percentage of recovered data. As known for SE-HSQC, signal intensity depends on the inter-pulse delays optimization, so in FID1 depends on Δ_1 , an in FID2 depends on Δ_1' (simulations are shown in Figure S4). As expected, FID1 affords the 50% of the SE-HSQC signal whereas the averaged intensity achieved in FID2 is about 35% when $\Delta_1' = \Delta_1 = 1/4$ J and about 25% when $\Delta_1' = 1/8$ J and $\Delta_1 = 1/4$ J (Figure 3C). As discussed before, this sensitivity reduction observed in FID2 is attributed to the unavoidable diffusion effects occurring during the duration of the FID1 period (about 100 ms). As shown later, this relative decrease of overall sensitivity concerning SE-HSQC is more than compensated with

the fact of being able to get multiple information into the same acquisition procedure and experimental times. On the other hand, it has been evaluated the diffusion losses as a function of the FID2 duration. In practice, the significant diffusion existing during a FID2 duration of 204 ms ($TD=2$ K) is partially compensated with the better resolution and linewidths (Figure S5).

Based on these descriptions, a family of new MFA experiments based on the MFA-HSQC/HSQC scheme can be designed. For instance, MFA-HSQCcoupled/HSQC and MFA-HSQC/HSQCcoupled experiments are readily available deactivating the heteronuclear decoupling during the FID1 or FID2, respectively (Figures S6–S9). Regarding overall sensitivity of both coupled and decoupled spectra, it can be recommended to acquire the coupled HSQC spectrum first in FID1 and the more sensitive decoupled HSQC in FID2 (Figures S8–S9). The same general scheme can also be applied for the simultaneous acquisition of a conventional HSQC and a broadband homodecoupled HSQC spectra (Figure 4B,C). Figure 4A shows the MFA-HSQC/psHSQC pulse scheme where the FID2 period is composed by a real-time BIRD-based homodecoupling acquisition scheme.^[27]

PEP has also proven its efficiency to enhance sensitivity in the HSQC-TOCSY experiment,^[17] by implementing an isotropic DIPSI2 mixing scheme at point b in SE-HSQC. The analysis of the involved components follows the same product operators described in Eq. 1, and therefore an MFA-HSQC/HSQC-TOCSY pulse scheme (Figure 5A) is advisable by incorporating the DIPSI pulse train before the FID2 period. A 2D HSQC spectrum is collected in FID1 whereas FID2 yields an HSQC-TOCSY spectrum, both with optional heteronuclear decoupling (Figure 5B).

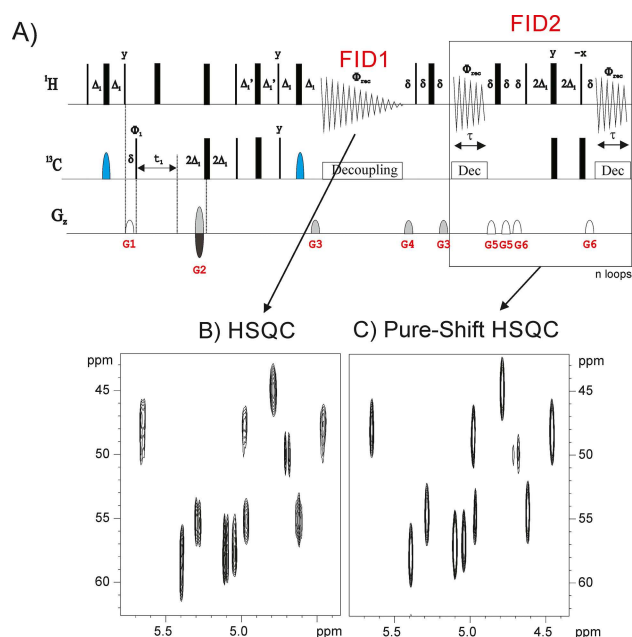


Figure 4. A) Pulse scheme of the MFA-HSQC/psHSQC experiment to acquire both regular and broadband homodecoupled HSQC spectra simultaneously; B–C) Expansions corresponding to the CH_α region of the B) multiplicity-edited HSQC and C) multiplicity-edited psHSQC spectra of cyclosporine, both acquired under identical conditions.

The relative signal loss observed in the second acquisition by diffusion is of the same order than described before for the HSQC experiment. As a further step, an MFA-HSQC-TOCSY/HSQC-TOCSY experiment is also feasible to collect two HSQC-TOCSY spectra with different mixing times (Figure S10). In this case, TOCSY transfer with DIPSI2 mixing periods of distinct duration is included before both FID1 and FID2 periods. Table S1 compares experimental times between regular HSQC and HSQC-TOCSY experiments and all their MFA counterparts. In general, it can be observed that MFA only extend about 7–12% the duration of the parent experiment.

In summary, a novel strategy to decipher the two active magnetization components involved in TOCSY and HSQC experiments has been described. The method affords multiple information content while offers optimized spectrometer times. Each magnetization component is monitored by independent FID periods into the same pulse sequence, providing two different NMR datasets with only an extension of 10% in the total acquisition time. The relative loss of signal observed in FID2 by diffusion effects does not affect the effectiveness of the method, which allows us to obtain a second experiment for free. The success of the method can be applied for different purposes, such as obtaining simultaneously two TOCSY or HSQC-TOCSY spectra with different mixing times or to acquire complementary HSQC spectra with various features (coupled vs decoupled; conventional vs pure shift, HSQC vs HSQC-TOCSY...). We anticipate that the combination of MFA methods with other time-optimized, resolution-enhanced and/or fast NMR techniques will further give rise the development of new experiments and better optimization of spectrometer times.

Experimental Section

NMR spectra were recorded on a Bruker AVANCE spectrometer equipped with a 5 mm TBI probehead operating at 600.13 MHz for ^1H at 298 K. The sample used in this work was 25 mM of cyclosporine dissolved in 0.6 ml of CDCl_3 . All MFA experiments were recorded using the same conditions and the echo/anti-echo protocol of the parents SE-TOCSY and SE-HSQC experiments. Basic parameters for the MFA-TOCSY/TOCSY experiment: The pre-scan delay was set to 1 s and 2 scans for each one of the 128 t_1 increments were acquired (1024 points of time domain in the acquisition dimension). The acquisition time of each FID1 and FID2 periods was of 102 ms. A basic two-step phase cycling was applied: $\Phi_1 = x, -x$; $\Phi_{\text{rec}} = x, -x$. The overall duration of the gradient (1 ms) and its recovery delay (δ) was 1.2 ms and the gradient ratio G1:G2 used was 30:23 (gradient shape SINE.100). A DIPSI-2 pulse train was used for TOCSY transfer, with mixing times set to 15 and 60 ms, respectively. All TOCSY experiments were acquired and processed using the echo/anti-echo protocol where the first gradient G1 was inverted for every second FID.

Similar conditions were used for the MFA-HSQC/HSQC and their related experiments. The inter-pulse delays were optimized to 145 Hz ($\Delta_1 = 1.72$ ms and $\Delta_1' = 0.86$ ms) and the gradient ratio G1:G2:G3:G4 was set to 17:80:20.1:33 (gradient shape SINE.100). A basic two-step phase cycling was applied: $\Phi_1 = x, -x$; $\Phi_{\text{rec}} = x, -x$. Real-time BIRD-based homodecoupling in MFA-HSQC/psHSQC was performed using 11.7 ms chunk length and 12 loops (2048 complex points in F_2). All MFA-HSQC experiments were acquired and

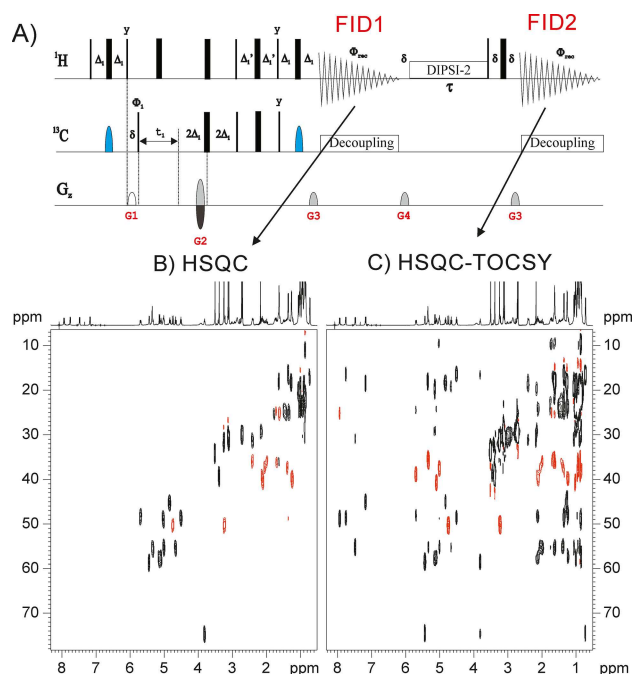


Figure 5. A) Pulse scheme of the MFA-HSQC/HSQC-TOCSY experiment. B) 2D multiplicity-edited HSQC and C) 2D multiplicity-edited HSQC-TOCSY ($\tau = 40$ ms) spectra of cyclosporine simultaneously acquired under identical conditions using the MFA-HSQC/HSQC-TOCSY pulse scheme.

processed using the echo/anti-echo protocol where the gradient G2 was inverted for every second FID.

Experimental times for all conventional and MFA-based TOCSY and HSQC experiments are shown in Table S1. Each FID1/FID2 is allocated in different memory blocks, and therefore all homonuclear and heteronuclear MFA datasets were individually processed in the usual way using the echo/anti-echo protocol. Zero-filling in both F1 and F2 dimensions, up 2048 and 1024 data matrix, respectively, and a non-shifted sine-bell window function in both dimensions were applied before Fourier transformation. All pulse programs are available in the SI.

Acknowledgements

Financial support for this research provided by Spanish MINECO (project CTQ2015-64436-P) is gratefully acknowledged. We also thank the Servei de Resonància Magnètica Nuclear, Universitat Autònoma de Barcelona, for allocating instrument time to this project.

Conflict of Interest

The authors declare no conflict of interest.

Keywords: HSQC • Multiple FID Acquisition • NMR spectroscopy • peptides • TOCSY

- [1] A. Z. Gurevich, I. L. Barsukov, A. S. Arseniev, V. F. Bystrov, *J. Magn. Reson.* **1984**, *56*, 471–478.
- [2] K. Motiram, M. Pérez-Trujillo, P. Nolis, T. Parella, *Chem. Commun.* in press **2018**, *54*, 13507–13510
- [3] P. Nolis, M. Pérez-Trujillo, T. Parella, *Angew. Chem. Int. Ed.* **2007**, *46*, 7495–7497.
- [4] Ě. Kupče, T. D. W. Claridge, *Angew. Chem. Int. Ed.* **2017**, *56*, 11779–11783; *Angew. Chem.* **2017**, *129*, 11941–11945.
- [5] Ě. Kupče, T. D. W. Claridge, *Chem. Commun.* **2018**, *54*, 7139–7142.
- [6] T. Parella, P. Nolis, *Concepts Magn. Reson. Part A* **2010**, *36*, 1–23.
- [7] Ě. Kupče, *Top. Curr. Chem.* **2013**, *335*, 71–96.
- [8] J. Cavanagh, M. Rance, *J. Magn. Reson.* **1990**, *88*, 72–85.
- [9] K. E. Kövér, D. Uhrin, V. J. Hruby, *J. Magn. Reson.* **1998**, *130*, 162–168.
- [10] G. Zhu, X. Kong, K. Sze, *J. Magn. Reson.* **1998**, *135*, 232–235.
- [11] X. M. Kong, K. H. Sze, G. Zhu, *J. Biomol. NMR* **1999**, *14*, 133–140.
- [12] L. E. Kay, P. Keifer, T. Saarinen, *J. Am. Chem. Soc.* **1992**, *114*, 10663–10665.
- [13] M. Sattler, M. G. Schwendinger, J. Schleucher, C. Griesinger, *J. Biomol. NMR* **1995**, *6*, 11–22.
- [14] J. Cavanagh, M. Rance, *Annu. Reports NMR Spectrosc.* **1993**, *27*, 1–58.
- [15] A. G. Palmer, J. Cavanagh, P. E. Wright, M. Rance, *J. Magn. Reson.* **1991**, *93*, 151–170.
- [16] J. Schleucher, M. Schwendinger, M. Sattler, P. Schmidt, O. Schedletzky, S. J. Glaser, O. W. Sørensen, C. Griesinger, *J. Biomol. NMR* **1994**, *4*, 301–306.
- [17] K. E. Kövér, V. J. Hruby, D. Uhrin, *J. Magn. Reson.* **1997**, *129*, 125–129.
- [18] R. T. Williamson, B. L. Márquez, W. H. Gerwick, *Tetrahedron* **1999**, *55*, 2881–2888.
- [19] S. S. Wijmenga, C. P. M. Van Mierlo, E. Steensma, *J. Biomol. NMR* **1996**, *8*, 319–330.
- [20] V. V. Krishnamurthy, *J. Magn. Reson. Ser. B* **1995**, *106*, 170–177.
- [21] K. Pervushin, R. Riek, G. Wider, K. Wüthrich, *Proc. Natl. Acad. Sci. USA* **1997**, *94*, 12366–12371.
- [22] D. Nietlispach, *J. Biomol. NMR* **2005**, *31*, 161–166.
- [23] J. Weigelt, *J. Am. Chem. Soc.* **1998**, *120*, 10778–10779.
- [24] M. Rance, J. P. Loria, A. G. Palmer, *J. Magn. Reson.* **1999**, *136*, 92–101.
- [25] D. R. Muhandiram, L. E. Kay, *J. Magn. Reson. Ser. B* **1994**, *103*, 203–216.
- [26] S. P. Rucker, A. J. Shaka, *Mol. Phys.* **1989**, *68*, 509–517.
- [27] L. Paudel, R. W. Adams, P. Király, J. A. Aguilar, M. Foroozandeh, M. J. Cliff, M. Nilsson, P. Sándor, J. P. Waltho, G. A. Morris, *Angew. Chem. Int. Ed.* **2013**, *52*, 11616–11619; *Angew. Chem.* **2013**, *125*, 11830–11833.

Manuscript received: November 7, 2018

Revised manuscript received: November 28, 2018

Version of record online: December 7, 2018